

Conference Paper, Published Version

Teles, Maria; Pires-Silva, António; Benoit, Michel

Development of a three-dimensional coupled system between TELEMAC-3D and TOMAWAC

Zur Verfügung gestellt in Kooperation mit/Provided in Cooperation with:
TELEMAC-MASCARET Core Group

Verfügbar unter/Available at: <https://hdl.handle.net/20.500.11970/104268>

Vorgeschlagene Zitierweise/Suggested citation:

Teles, Maria; Pires-Silva, António; Benoit, Michel (2014): Development of a three-dimensional coupled system between TELEMAC-3D and TOMAWAC. In: Bertrand, Olivier; Coulet, Christophe (Hg.): Proceedings of the 21st TELEMAC-MASCARET User Conference 2014, 15th-17th October 2014, Grenoble – France. Echirolles: ARTELIA Eau & Environnement. S. 11-17.

Standardnutzungsbedingungen/Terms of Use:

Die Dokumente in HENRY stehen unter der Creative Commons Lizenz CC BY 4.0, sofern keine abweichenden Nutzungsbedingungen getroffen wurden. Damit ist sowohl die kommerzielle Nutzung als auch das Teilen, die Weiterbearbeitung und Speicherung erlaubt. Das Verwenden und das Bearbeiten stehen unter der Bedingung der Namensnennung. Im Einzelfall kann eine restriktivere Lizenz gelten; dann gelten abweichend von den obigen Nutzungsbedingungen die in der dort genannten Lizenz gewährten Nutzungsrechte.

Documents in HENRY are made available under the Creative Commons License CC BY 4.0, if no other license is applicable. Under CC BY 4.0 commercial use and sharing, remixing, transforming, and building upon the material of the work is permitted. In some cases a different, more restrictive license may apply; if applicable the terms of the restrictive license will be binding.



Development of a three-dimensional coupled system between TELEMAC-3D and TOMAWAC

Maria João Teles^{1,2}, António A. Pires-Silva²

¹Antea Group
Ghent, Belgium

²Instituto Superior Técnico, ULisboa
Lisboa, Portugal
mjteles@gmail.com

Michel Benoit³

³Saint-Venant Hydraulics Laboratory (EDF R&D,
CEREMA, ENPC)
Chatou, France

Abstract — A two-way coupled system between the hydrodynamic model TELEMAC-3D and the spectral wave model TOMAWAC was developed in order to get the three-dimensional description of waves and current interaction effects. The mathematical framework is based on the recent work presented by [2] in which the glm2z-RANS equations are deduced. First, the coupled system was tested against an academic test case [3]. Then in order to analyse and validate the numerical results of nearshore circulation, two sets of laboratory measurements were used: one on a planar beach [7] and another one on a barred beach [6].

I. INTRODUCTION

Within the coastal waters there are a number of processes that have distinct temporal and spatial scales. Their interaction renders the description of nearshore hydrodynamics rather complex. The combined environment of waves and currents provides one example of those interactions. In the nearshore area the wave breaking and the induced generated currents, such as longshore and rip currents, can create a dangerous environment for humans and have a great impact on morphodynamics.

For many years the radiation stress concept [9] was largely used within a two-dimensional approach to analyse the above mentioned combined flow. Nevertheless, in the past decade it has been shown that the three-dimensional effects of waves and current interactions are essential to get a correct description of these phenomena. A number of authors proposed different ways of approaching this problem. Two main groups can be distinguished regarding the theoretical framework: either the radiation stress concept is used [11] or a vortex force approach is applied [10], [2].

[2] chose to work with the set of GLM equations [1] in which there is a clear distinction between the oscillatory and the mean motion. They were able to get second order expressions for the wave forcing terms needed to close the GLM equations. Through a change in the vertical GLM coordinates to Cartesian coordinates they obtained the so-called glm2z-RANS equations. With this theory the description of the interaction effects between waves and currents can be achieved throughout the entire water depth.

In the present work the glm2z-RANS equations were used to develop a new coupled system between a hydrodynamic circulation model and a spectral wave model. The TELEMAC-MASCARET numerical platform was the chosen tool to work with. The new equations were implemented in the three-dimensional model TELEMAC-3D [8] together with new boundary conditions. New parameterizations were incorporated in the models to compute the wave forcing terms. The later are calculated by the spectral wave model TOMAWAC [4] and passed to TELEMAC-3D by internal coupling.

Firstly, in order to test the coupled system, it was performed an academic test case based on the adiabatic test presented by [3]. Secondly, laboratory data was used to verify the numerical results and study the three-dimensional effects of waves and currents interaction. There were available measurements from two different wave-basin configurations: one on a planar beach [7], where wave induced longshore currents were reproduced, and another, on a barred beach [6], in which a rip current system was generated.

A description of the mathematical formulation developed in TELEMAC-3D together with an explanation of the practical implementation of the coupling made with TOMAWAC is given in the following section. On section III the numerical results obtained with the adiabatic test case are presented. Section IV shows the comparisons between numerical output and measurements for the two test cases of wave induced nearshore circulation. On section V some concluding remarks are highlighted.

II. COUPLING SYSTEM

A. Governing equations

As already mentioned TELEMAC-3D was the chosen model. To take into account the three-dimensional effects of the combined environment new wave forcing terms had to be introduced. With that aim the mathematical framework proposed by [2], the glm2z-RANS equations, were implemented. Following [3] the vertical current shear was neglected in the wave forcing terms.

The equations of mass (1) and horizontal momentum conservation (2) considering an incompressible fluid and the hydrostatic assumption are

$$\frac{\partial \hat{u}_\alpha}{\partial x_\alpha} + \frac{\partial \hat{w}}{\partial z} = 0 \quad (1)$$

$$\begin{aligned} \frac{\partial \hat{u}_\alpha}{\partial t} + \hat{u}_\beta \frac{\partial \hat{u}_\alpha}{\partial x_\beta} + \hat{w} \frac{\partial \hat{u}_\alpha}{\partial z} = S_{x\alpha} - g \frac{\partial \hat{\eta}}{\partial x_\alpha} + \\ + \frac{\partial}{\partial x_\beta} \left(\nu_H \frac{\partial \hat{u}_\alpha}{\partial x_\beta} \right) + \frac{\partial}{\partial z} \left((\nu_z + \nu_{wbz}) \frac{\partial \hat{u}_\alpha}{\partial z} \right) - \\ - \epsilon_{\alpha\beta\gamma} (f_3 + \omega_3) U_{\beta s} - W_s \frac{\partial \hat{u}_\alpha}{\partial z} - \frac{\partial J}{\partial x_\alpha} \end{aligned} \quad (2)$$

$(\hat{u}_\alpha, \hat{w})$ represent the quasi-Eulerian velocities given, in a second order approach, by the difference between the Lagrangian mean velocities and the Stokes drift $(U_{\alpha s}, W_s)$. The acceleration due to gravity is given by g and S_x represents the hydrodynamic model horizontal source terms, for instance, the Coriolis force. ν_H and ν_z are, respectively, the horizontal and vertical and turbulence viscosities. The viscosity values can either be prescribed by the user or computed by a turbulence closure model. Furthermore, within the wave-current environment and due to wave breaking there is an enhancement of the vertical mixing. To take into account this effect the formulation proposed by [14] was followed implying that a wave-enhanced vertical mixing (ν_{wbz}) is added to the vertical turbulence viscosity.

The new wave forcing terms included in the hydrodynamic model momentum equations are the Stokes drift, the horizontal gradient of the wave-induced pressure (J), the vortex force in x_α , which is represented in $\epsilon_{\alpha\beta\gamma} \omega_3 U_{\beta s}$ (defined by the vectorial product between the mean flow vertical vorticity ω_3 and the horizontal Stokes drift) and the stokes-Coriolis force represented by $\epsilon_{\alpha\beta\gamma} f_3 U_{\beta s}$.

To guarantee mass conservation, the mass induced by the Stokes drift in the depth-integrated continuity equation (3) was included. The symbol $(\bar{\cdot})$ denotes a depth-integrated variable.

$$\frac{\partial h}{\partial t} + \frac{\partial h \bar{u}_\alpha}{\partial x_\alpha} = - \frac{\partial h \bar{W}_{\alpha s}}{\partial x_\alpha} \quad (3)$$

Moreover, the bottom shear stress in the hydrodynamic model was modified in order to take into account the wave-current interaction effects on the bottom roughness, following the [5]'s theoretical framework.

At the offshore open boundary two conditions are imposed for the phase-averaged elevation (4) and the horizontal velocities (5) [12]:

$$\hat{\eta} = -J/g \quad (4)$$

$$\hat{u}_\alpha = -U_{\alpha s} \quad (5)$$

The momentum lost by waves due to depth-induced wave breaking and bottom friction was imposed in the hydrodynamic model as free surface and bottom stresses, respectively. These non-conservative wave forcing effects were included and calculated in the wave model. TOMAWAC v6.p2 [4], a third generation spectral wave model, was the chosen model. It solves the wave action (N) conservation equation in Cartesian (x, y) or spherical spatial coordinates and the domain is discretized in unstructured grids.

B. Implementation

In the following, it is given a brief explanation to describe how the coupled system works (Figure 1).

TELEMAC-3D starts the calculation. The Nikuradse roughness, the z-levels, and the computed depth-integrated velocities and mean surface elevation are communicated to TOMAWAC. In its turn, the wave model computes, over a time step, the wave forcing terms: the Stokes drift components, the wave-induced pressure, the wave breaking and the bottom-induced dissipation momentum contributions. The last two terms are imposed as surface and bottom stresses, respectively, in the hydrodynamic model. Furthermore, the wave model calculates the wave-enhanced vertical mixing coefficient that is added to the vertical turbulence viscosity in TELEMAC-3D. This process is repeated each time step or made within a coupling period defined by the user. The coupling period between TELEMAC-3D and TOMAWAC can be larger than the time step of the models. The time step of each of the models does not have to be the same, just a multiple of each other. Both models run with the same horizontal mesh.

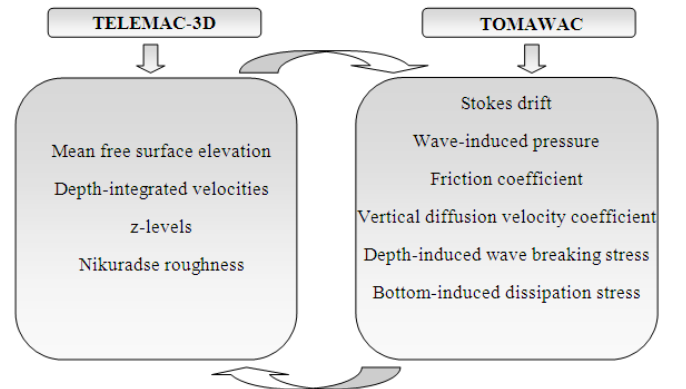


Figure 1. Scheme of the different terms computed and exchanged by TELEMAC-3D and TOMAWAC

III. ACADEMIC TEST CASE

In order to test the implementation of the glm2z-RANS equations in the coupled system TELEMAC-3D and TOMAWAC it was performed an academic test case presented by [3]. It is an adiabatic case with monochromatic waves propagating over a step that evolves from 6 m to 4 m depth (Figure 2). As no dissipation occurs the flow generated by the propagating waves over the bottom slope can be considered irrotational.

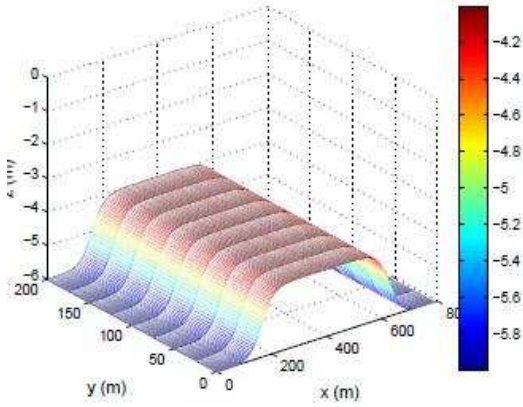


Figure 2. Bathymetry representation for the adiabatic test. The colour scale represents the bottom elevation (m).

The upstream ($x = 0$ m) and downstream ($x = 800$ m) boundaries are defined as open boundaries where the mean sea surface is zero and condition (5) is applied for the velocities. The horizontal mesh was discretized with elements of triangular basis of 5 m in x direction and 25 m in y direction. The hydrodynamic model was run with 10 horizontal planes equally spaced throughout the water depth. In TOMAWAC, a monochromatic wave was imposed with wave height $H = 1.02$ m and wave period $T = 5.26$ s. The waves propagate along the positive x axis. Sources and sink terms are deactivated both in TELEMAC-3D and TOMAWAC. The time step chosen for the hydrodynamic model was 0.2 s while for the wave model was 2 s. The models run until stationarity was achieved.

On Figure 3 it is possible to verify the wave height evolution over the domain. Due to the bottom slope the waves shoal increasing the wave amplitude and inducing a mass transport in the shallower part of the domain (Figure 4). To compensate the divergence of the Stokes drift a mean steady current is generated with opposing direction to the propagating waves (Figure 5).

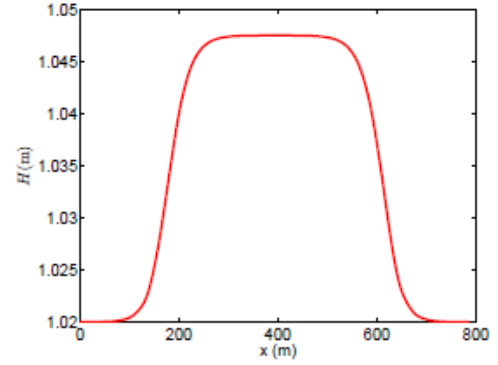


Figure 3. Wave height evolution. Incident wave height $H = 1.02$ m and peak wave period $T = 5.26$ s.

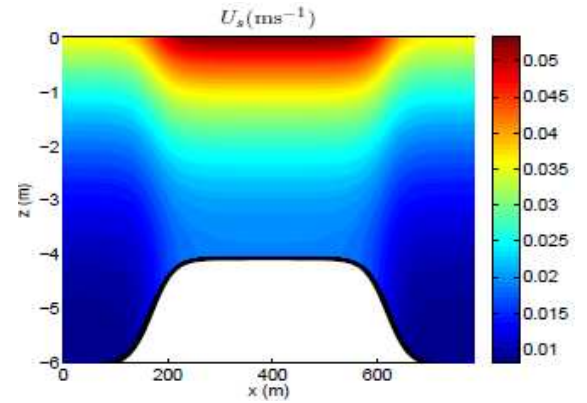


Figure 4. Horizontal Stokes velocity evolution. Incident wave height $H = 1.02$ m and wave period $T = 5.26$ s

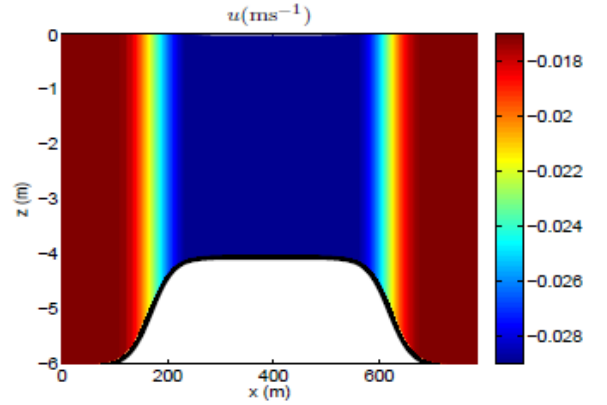


Figure 5. Horizontal quasi-Eulerian velocity evolution. Incident wave height $H = 1.02$ m and wave period $T = 5.26$ s

As there are no source or sink terms in the domain and the mean current vertical shear is weak, the evolution of the horizontal velocity by itself (Figure 6) is equal to the contribution of wave induced pressure gradient (Figure 7) together with hydrostatic pressure gradient (Figure 8). The variables represented in the figures below are computed and given as an output by the coupled system, showing this particular momentum balance.

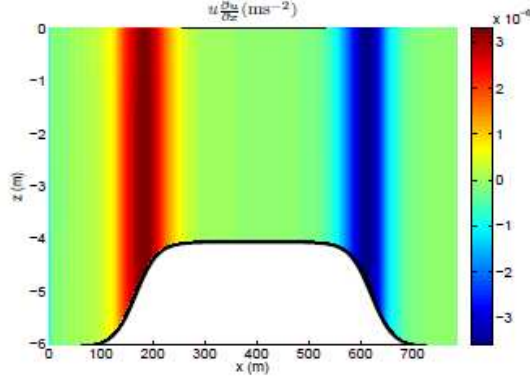


Figure 6. Evolution of the velocity advection by itself

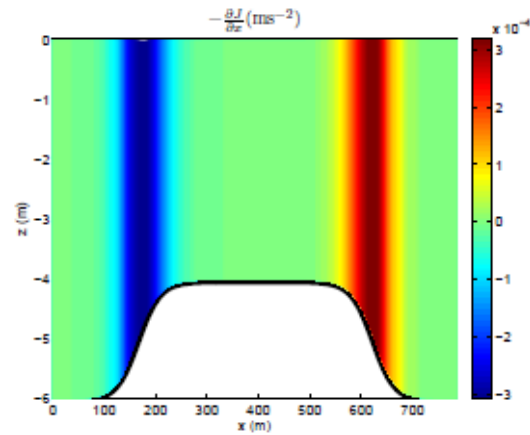


Figure 7. Evolution of the wave induced pressure horizontal gradient

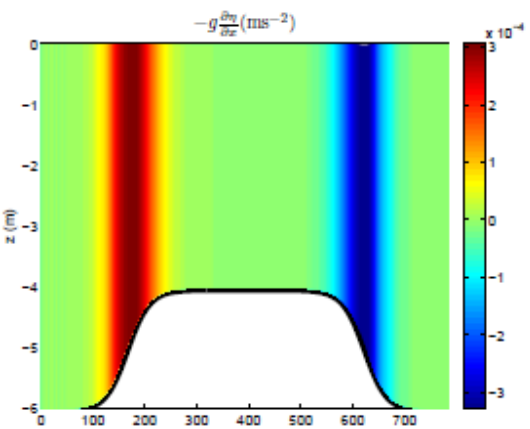


Figure 8. Evolution of the hydrostatic pressure horizontal gradient

IV. NEARSHORE CIRCULATION

A. Planar beach

Wave induced longshore currents can play an important role in different situations, as in nearshore morphodynamics. Therefore it is important to model and study properly their dynamics.

In this section the modified equations implemented in the coupled system are tested against measurements obtained on a laboratory wave basin. The main purpose of the experiment was to reproduce the wave-induced longshore currents generated by obliquely incident breaking waves on a planar beach [7]. The facility has approximately 30 m x 50 m, a slope of 1:30 in the main section and 1:18 at the toe of the beach. A pumping system was installed in the lateral walls aiming to ensure longshore uniformity of the currents. Four wave paddles generate irregular waves with an incident angle of 10° relative to the beach, a significant wave height of $H_s = 0.225$ m and a wave peak period of $T_p = 2.5$ s. The bottom was made of concrete. Values of surface elevation and velocities were obtained by ten capacitance type wave gauges and ten Acoustic-Doppler Velocimeters (ADVs), respectively, which were co-located along a cross-shore direction of the wave basin.

The computational domain was discretized with $\Delta x = 0.2$ m and $\Delta y = 0.8$ m. Ten horizontal planes were distributed uniformly throughout the water depth in TELEMAC-3D. The time step was set to $\Delta t = 0.2$ s for both hydrodynamic and wave models. The offshore boundary conditions were defined with expressions (4) and (5) and the lateral boundaries characterized with periodic conditions in order to ensure the longshore uniformity of the wave generated currents. The Nikuradse roughness was set to $k_s = 0.0001$ m. The chosen turbulence model was the $k-\epsilon$ LP (Linear Production) model that computes the vertical turbulence viscosity. The horizontal turbulence viscosity value was set to $\nu_h = 0.2 \text{ m}^2 \text{ s}^{-1}$. The Coriolis force is neglected.

To model wave propagation a JONSWAP spectrum with a peak enhancement factor of $\gamma = 7$ was imposed. The significant wave height and the wave period were the same as the ones used in the laboratory experiments. The spectral domain was discretized with 25 frequencies with the minimum frequency equal to 0.1 Hz and the frequency ratio $q = 1.07$. For the depth-induced wave breaking the [13]'s model was chosen with the parameters $B = 1.25$ and $\gamma = 0.75$. Both effects of waves on the current and of the current on the propagation of waves were taken into account. The model ran continuously until a stationary state was achieved.

On Figure 9 the comparison between results computed by the coupled system and experimental data for the evolution of the significant wave height is shown. It can be seen that the model fits well the measurements along a cross-shore section from offshore to the beach.

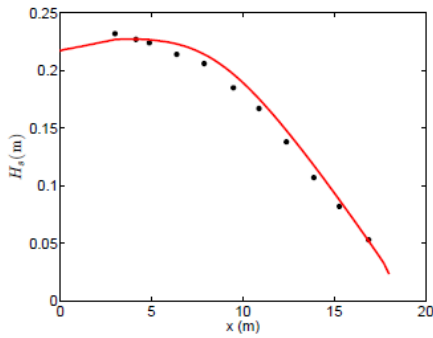


Figure 9. Comparison between numerical results (line) and experimental data (dots) of the significant wave height along a cross-shore section of the wave basin ($y = 27$ m)

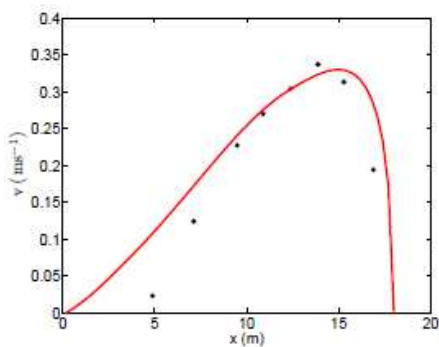


Figure 10. Comparison between numerical results (line) and data (dots) of the longshore velocity at one third of the water depth

On Figure 10 the longshore velocity measured at one third of the water depth is compared to the one computed by TELEMAC-3D/TOMAWAC. It can be verified that not only the evolution along a cross-shore section ($y = 27$ m) but also the magnitude of the computed velocity agrees well with the measurements. The differences observed in the offshore part of the domain are probably due to the fact that in the laboratory basin some difficulties were found to control an internal and spurious recirculation that occur near the wave paddles.

On Figure 11 the cross-shore (above) and longshore (below) velocity vertical profiles are represented along a cross-shore transect $y = 27$ m. When approaching the beach the cross-shore velocities show an important shear from the bottom to the free surface, evidencing the importance of taking into account the three-dimensional effects of waves and current interactions. The longshore velocity vertical shear is not so relevant but the magnitude is almost three times the values of the cross-shore velocities.

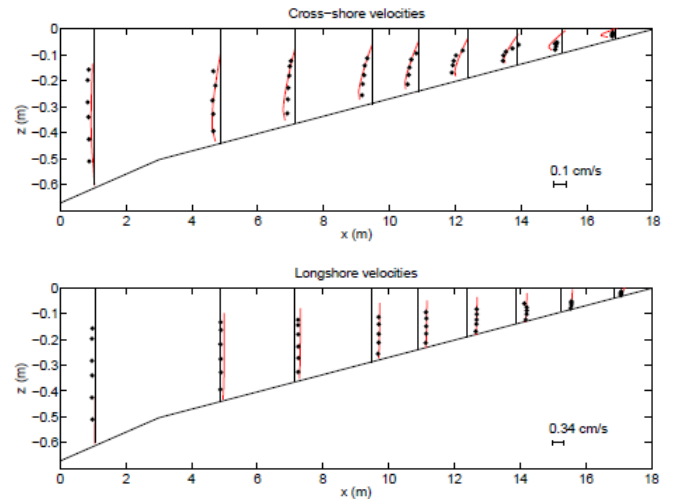


Figure 11. Comparison of numerical results (lines) with experimental data (dots) of cross-shore (above) and longshore (below) velocity vertical profiles along a cross-shore transect $y = 27$ m

B. Barred beach

In the present section the capability of the coupled system to model rip currents is tested. Measurements obtained in a laboratory wave basin [6] were used to validate the numerical results. Here the bathymetric contour lines are no longer parallel to the coastline, but instead there are two bars which induce wave breaking and the generation of a rip current system. The wave basin is 17.2 m in the cross-shore direction and 18.7 m in the longshore direction. The slope is 1:5 from offshore up to three meters from the wave maker and then 1:30 till the end of the beach. The generated waves were monochromatic and perpendicular to the beach. The vertical structure of rip currents was assessed through the installation of three Sontek Acoustic Doppler Velocimeters. [6] measured the vertical structure of the rip currents and applied a bin average technique to analyse the data. The bin is a categorization of the data, sorted by the velocities measured at the top the water column (u_1). This implicit scale is defined by intervals of the referred velocities values. The criteria used were: bin 25 ($u_1 > 0.25$ (ms^{-1})), bin 20 ($0.25 > u_1 > 0.20$ (ms^{-1})), bin 15 ($0.10 > u_1 > 0.15$ (ms^{-1})) and bin 10 ($0.15 > u_1 > 0.10$ (ms^{-1})).

The computational domain was discretized equally for both models with $\Delta x = \Delta y = 0.2$ m (Figure 12). In the z direction eight horizontal planes were defined for TELEMAC-3D.

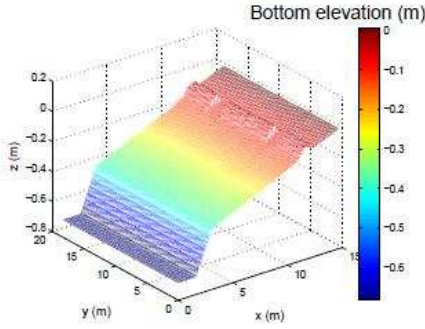


Figure 12. Computational domain for the rip current test case

The time step was set to $\Delta t = 0.03$ s for both hydrodynamic and wave models. Conditions (4) and (5) were once more assigned at the offshore boundary and walls were defined at lateral and shoreward boundaries. The Nikuradse roughness was set to $k_s = 0.01$ m. The $k-\epsilon$ model was the chosen turbulence model to compute the vertical turbulence viscosity. A value of $\nu_H = 0.001 \text{ m}^2 \text{ s}^{-1}$ was set for the horizontal turbulence viscosity. The numerical simulations with TOMAWAC were performed with spectral parameters that match the monochromatic laboratory experiments. This way, a significant wave height was set to $H_s = 0.067$ m. The minimum frequency was set to 0.187 Hz, the number of frequencies to 7 and the frequential ratio to 1.4. The directional discretization was made through 24 direction bins. For the depth-induced breaking the model proposed by [13] was chosen with $\gamma = 0.9$ and $B = 1$.

The comparison between numerical results obtained by the coupled system and the measurements made along the cross-shore section $y = 13.6$ m are depicted on Figure 13. The upper panel, relative to bin10, shows how the rip current vertical structure evolves from offshore to the beach. Offshore the domain, the cross-shore velocity increases from the bottom up to the free surface. It can be observed that the model has difficulties in modelling the current in this area, overestimating the velocities. From $x = 11$ m until the shoreline the velocity reaches its maximum below the bar-crest level and starts to slightly decrease near the free surface. The vertical distribution of the cross-shore velocities is quite well represented by the numerical model, mostly in the vicinity of the rip channel.

The lower panel of Figure 13 shows that the magnitude of these rip currents can attend high values and that the model is able to capture them.

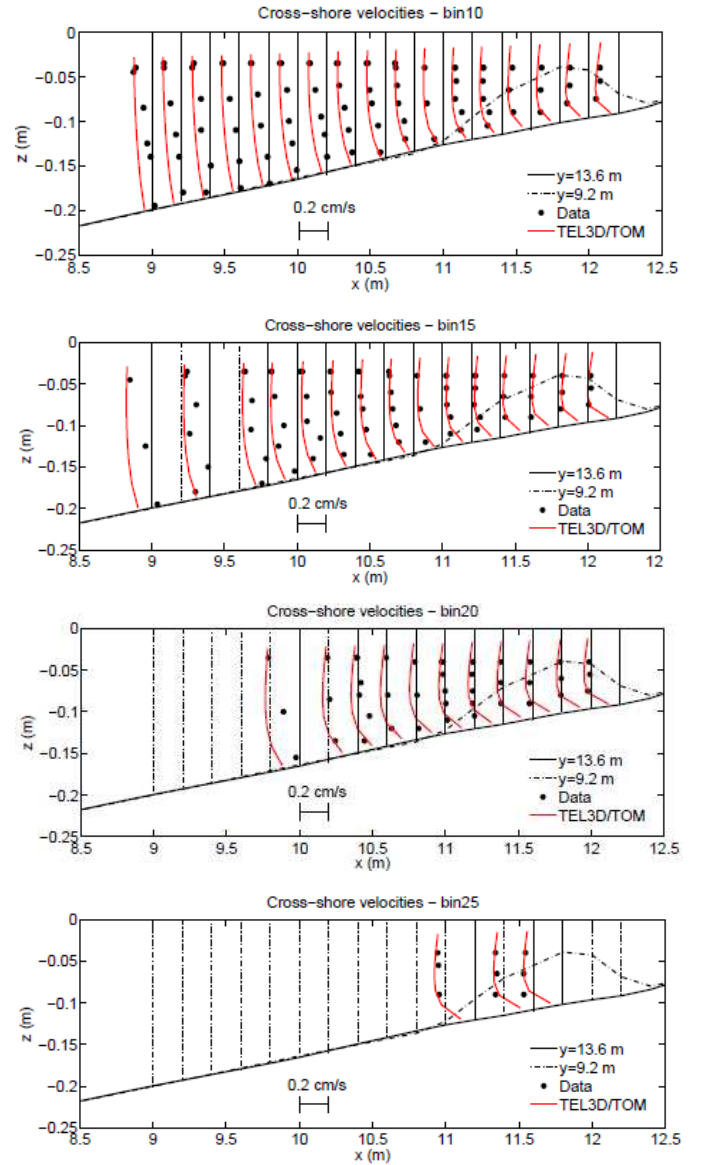


Figure 13. Comparison of the cross-shore velocity vertical profiles through the rip channel from numerical model and from experimental data [6] within bins 10, 15, 20 and 25. The full vertical lines represent the measurement sections.

V. CONCLUDING REMARKS

A new coupled system between the three-dimensional hydrodynamic model TELEMAC-3D and the spectral wave model TOMAWAC was developed. The glm2z-RANS equations [2] were implemented in the numerical model together with the simplifications proposed by [3]. New parameterizations were included in order to calculate the wave forcing terms.

An adiabatic test case presented in [3] was made in order to test the coupled system. Then, measurements obtained in two laboratory basins with different set ups were compared with numerical results. Firstly longshore currents induced by waves breaking on a planar beach were modelled. Then a second test was performed, which consisted in reproducing a

rip current system generated by waves breaking on a barred beach. Numerical results were in good agreement with laboratory data showing the capability of the coupled system to model, at least at this scale, waves and current interactions in the nearshore area.

ACKNOWLEDGEMENT

Maria João Teles would like to acknowledge the support of a PhD grant (SFRH/BD/61269/2009) from FCT (Fundação para a Ciência e Tecnologia), Portugal. The authors would also like to acknowledge all the support given by the TELEMAC-MASCARET development team.

REFERENCES

- [1] Andrews, D. G., McIntyre, M. E., 1978a. An exact theory of non linear waves on a Lagrangian mean flow. *Journal of Fluid Mechanics*, Vol. 89, pp 609-646.
- [2] Ardhuin F., Rascle N., Belibassakis K.A. (2008). Explicit wave-averaged primitive equations using a generalized Lagrangian mean. *Ocean Modelling*, Vol. 20(1), pp 35-60
- [3] Bennis A.-C., Ardhuin F., Dumas F. (2011). On the coupling of wave and three-dimensional circulation models: Choice of theoretical framework, practical implementation and adiabatic tests. *Ocean Modelling*, Vol. 40(3-4), pp 260-272
- [4] Benoit M., Marcos F., Becq F. (1996). Development of a third generation shallow water wave model with unstructured spatial meshing. *Proc. 25th Int. Conf. on Coastal Eng. (ICCE'1996)*, 2-6 September 1996, Orlando (Florida, USA), pp 465-478
- [5] Christoffersen, J. B., Jonsson, I. G., 1985. Bed friction and dissipation in a combined current and wave motion. *Ocean Engineering*, Vol. 12, pp 387-949 423.
- [6] Haas, K. A., Svendsen, I. A. (2002). Laboratory measurements of the vertical structure of rip currents. *Journal of Geophysical Research*, Vol. 107 (C5), 3047
- [7] Hamilton, D. G., Ebersole, B. A., 2001. Establishing uniform longshore currents in a large scale sediment transport facility. *Coastal Engineering*, Vol. 42, pp 199-218.
- [8] Hervouet J.-M. (2007) *Hydrodynamics of free surface flows, modelling with the finite element method*. Editions Wiley & Sons. ISBN 978-0-470-03558, 342 p.
- [9] Longuet-Higgins, M. S., Stewart, R. W., 1962. Radiation stress and mass transport in gravity waves, with applications to surf beats. *Journal of Fluid Mechanics*, Vol. 13, pp 481-504.
- [10] McWilliams, J. C., Restrepo, J. M., Lane, E. M., 2004. An asymptotic theory for the interaction of waves and currents in coastal waters. *Journal of Fluid Mechanics*, Vol. 511, pp 135-178.
- [11] Mellor, G., 2003. The Three-Dimensional Current and Surface Wave Equations. *Journal of Physical Oceanography*, Vol.33, pp 1978-1989.
- [12] Rascle, N., 2007. Impact of waves on the ocean circulation. PhD thesis, Université de Bretagne Occidentale, France.
- [13] Thornton, E. B., Guza, R. T., 1983. Transformation of wave height distribution. *Journal of Geophysical Research*, Vol. 88 (C10), pp 5925-5938.
- [14] Uchiyama, Y., McWilliams, J. C., Shchepetkin, A. F., (2010). Wave-current interaction in an oceanic circulation model with a vortex-force formalism: Application to the surf zone. *Ocean Modelling*, Vol. 34, pp 16-35